processes

MDPI

Article

NIR-Based Real-Time Monitoring of Freeze-Drying Processes: Application to Fault and Endpoint Detection

Ambra Massei [1,2], Nunzia Falco [2] and Davide Fissore [1,*]

[1] Dipartimento di Scienza Applicata e Tecnologia, Politecnico di Torino, Corso Duca degli Abruzzi 24, 10129 Torino, Italy; ambra.massei@merckgroup.com
[2] Global Parenteral Development, Merck Serono S.p.A., Via Luigi Einaudi 11, Guidonia Montecelio, 00012 Roma, Italy; nunzia.falco@merckgroup.com
* Correspondence: davide.fissore@polito.it

Abstract: In the pharmaceutical industry, freeze-drying is crucial for the stability of active pharmaceutical ingredients (APIs). Monitoring this complex process presents challenges as traditional methods often lack real-time insights, potentially leading to quality issues and batch rejections. Effective monitoring is then essential for optimizing process parameters and minimizing waste, thus saving costs and resources. This study evaluated the application of Near-Infrared (NIR) spectroscopy for the real-time monitoring of the freeze-drying process: NIR spectra were acquired in-line via a specially designed flange in the freeze-dryer. Two approaches were investigated. The first involved freeze-drying monitoring using control charts, thus creating a reference model based on cycles under normal conditions. A PCA model was developed using these reference cycles, and an intentional fault cycle was performed to test the system's ability to detect deviations. Multivariate control charts, utilizing Hotelling's T^2 and DModX metrics, were shown to effectively monitor process deviations, enhancing the understanding of freeze-drying dynamics. The second approach was based on the use of NIR spectroscopy for assessing residual moisture during lyophilization. By integrating Partial Least Squares (PLS) regression with in-line NIR spectra, we estimated endpoints and detected faults in both reference and faulty cycles. The results showed strong correlations between PLS estimates and the Pirani–Baratron method, highlighting NIR's applicability for monitoring drying phases. This research advocates for broader NIR implementation in pharmaceutical development, emphasizing its potential to monitor the process, ensure quality, and reduce out-of-specification product.

Keywords: NIR spectroscopy; process analytical technology; freeze-drying; biopharmaceuticals; monitoring

Academic Editors: Athanasia Varvaresou and Chunhui Zhao

Received: 16 December 2024
Revised: 21 January 2025
Accepted: 5 February 2025
Published: 7 February 2025

Citation: Massei, A.; Falco, N.; Fissore, D. NIR-Based Real-Time Monitoring of Freeze-Drying Processes: Application to Fault and Endpoint Detection. *Processes* **2025**, *13*, 452. https://doi.org/10.3390/pr13020452

1. Introduction

Batch processes are widely used across different sectors, including chemical, pharmaceutical, food and biotechnology industries. Specifically, the finished product manufacturing relies, in most cases, on batch processes, defined by a limited duration and non-steady-state behavior. In this case, when a batch run is successfully completed during the development phase and yields a product that meets specifications, the key process variables from that run are documented in a recipe. Then, the latter is employed for future batch productions, aiming to guarantee, by this way, the product quality. However, it is

not always sufficient to apply a recipe-driven approach to guarantee product quality, as several deviations may occur in the process, due to equipment failures and/or the effect of non-controlled variables (disturbances) on the process. Therefore, monitoring in real-time a specific process is mandatory. Additionally, this offers other benefits, including the possibility of a real time optimization and a deeper understanding of the process itself [1].

Pharmaceutical companies are encouraged to focus on reducing Research and Development (R&D) costs [2]. In this framework, the Food and Drug Administration (FDA) is encouraging the introduction of new technologies aimed to gain a deeper understanding of the pharmaceutical processes in the perspective of the Quality by Design (QbD) on the contrary of the Quality by Testing (QbT) approach [3]. This approach emphasizes embedding product quality within the production process rather than solely testing it at the end of the manufacturing [4]. According to QbD approach, it would be optimal to monitor in real-time the Drug Product (DP) manufacturing process and the related Critical Quality Attributes (CQAs), allowing for intervention in case of issues [5]. These aims can be reached using suitable Process Analytical Technology (PAT) tools, such as Near-Infrared or Raman spectroscopy [6].

One of the most critical and expensive steps in Drug Product development and manufacturing is the freeze-drying process. It allows for water removal guaranteeing the stability of the active pharmaceutical ingredient (API) by converting the liquid formulation in a solid-state form. In such a way, chemical and physical degradation processes are prevented. Three steps are involved in a freeze-drying cycle. Initially, the solution undergoes freezing to transform the liquid solvent into ice. Subsequently, ice crystals sublimate under low-temperature and pressure conditions during the primary drying phase, resulting in the formation of a solid porous structure, called "cake". Finally, in the secondary drying stage, the temperature is raised to facilitate the desorption of bound water, i.e., the amount of water that did not turn into ice in the freezing stage. At the end of a lyophilization cycle, different CQAs, like residual moisture (RM), protein aggregation level, potency and purity, must be tested to meet the product specification [7]. Usually, few samples are analyzed due to the destructive and time-consuming analysis currently employed to measure the CQAs. Unfortunately, this approach does not provide a clear understanding of the freeze-drying process due to the intrinsic heterogeneity nature of the process itself. In fact, pressure differences among the shelves, inconsistencies in surface temperatures and varying radiative heat received by the vials in the drying chamber are key factors that lead to intra-batch heterogeneity, thus posing issues on the representativeness of the monitored vials [8,9].

The real-time monitoring of the freeze-drying process could allow for a deeper understanding of this process that can be used to optimize or adjust the process while it is occurring, avoiding the rejection of a full batch in case of deviations of the operating conditions from the target one. In fact, the prompt and accurate identification of potential faults during the process can enable timely corrections before the entire batch is compromised, thereby minimizing both the failure rate and waste generation [10]. If the product is confirmed to be produced from a controlled process, the number of required assays and the time needed for batch release can be significantly decreased from a statistical perspective. Additionally, given that the primary drying phase of a pharmaceutical product can extend over several days or even weeks, it is crucial to assess whether a batch is deviating from its designated parameters, allowing for prompt intervention before further time is lost [11]. This approach can be effectively utilized in Stage 3 of process validation activities where continuous process verification (CPV) is essential. By implementing real-time monitoring techniques, manufacturers can ensure that the freeze-drying process remains within predefined control limits throughout production. This proactive monitoring not only supports compliance with regulatory standards but also enhances overall process

reliability and product quality, ultimately leading to more efficient manufacturing practices and improved patient safety.

In this framework, Near-Infrared spectroscopy (NIR) can be a powerful tool due to its non-destructive nature and its high sensitivity to water [12]. In fact, it relies on the measurement of the absorbance related to vibrational transitions in molecules by focusing on the Near-Infrared region of the electromagnetic spectrum [13]. NIR spectroscopy has been widely investigated as a tool to quantify residual moisture content in freeze-dried products [14,15]. Bobba et al. [16] and Massei et al. [17] developed different algorithms, based on Partial Least Squares (PLS) and the Artificial Neural Network (ANN), to estimate residual moisture content in different surrogate-based solutions. Jones et al. demonstrated that NIR models, developed independently at two locations for non-invasive moisture measurement in freeze-dried products, can effectively use calibration equation from one site to accurately predict moisture content in products manufactured at the other site [18]. Other works aiming to evaluate RM starting from NIR spectra can be found in the literature [19,20].

Although process monitoring in the pharmaceutical industry has historically been conducted in a univariate manner, prioritizing quality assurance over fault analysis, recent advancements have introduced more sophisticated routines for fault detection and identification within pharmaceutical processes. These methods are based on multivariate statistical process control (MSPC) [21]. As an example, Kirdar et al. demonstrated the effectiveness of MSPC charts for fault detection in routine manufacturing within a cell culture operation [22]. García-Muñoz and Settel evaluated MSPC in a pilot-scale spray-drying process, finding the monitoring system to be effective for fault diagnosis [23]. However, NIR spectroscopy has been poorly investigated as an in-line tool to monitor the freeze-drying process. As an example, Kona et al. introduced an MSPC system coupled with in-line NIR spectroscopy aimed at identifying faults in a batch fluid bed granulation process [24]. De Beer et al. investigated the complementary capabilities of Raman and NIR spectroscopy for in-line monitoring, demonstrating that both techniques can provide critical insights into various physical and chemical phenomena throughout the process. Specifically, NIR was used to monitor the endpoint of ice sublimation and hydrate water release [25]. Also, Rosas et al. demonstrated that NIR spectroscopy could effectively monitor physiochemical changes, including crystallization behavior and solvent sublimation by monitoring a multi-component pharmaceutical formulation during freeze-drying [26].

From this overview, it appears that while NIR spectroscopy has been extensively studied for quantifying residual moisture content in freeze-dried products, its application as an in-line tool for monitoring the freeze-drying process has been poorly explored. Currently, freeze-drying is monitored only at the end of the cycle by evaluating specific CQAs such as residual moisture, appearance and protein content using time-consuming and ineffective laboratory techniques. This traditional approach not only leads to the waste of both material and time but also poses significant risks as it is not possible to address or mitigate issues without potentially discarding the entire batch.

In contrast, the integration of multivariate statistical process control methods into the freeze-drying process represents a significant innovation in the pharmaceutical field. This advancement is particularly relevant for excipients commonly found in biopharmaceutical formulations as it aligns with the principles of Quality by Design (QbD). By implementing real-time monitoring and control, manufacturers can gain immediate insights into the process, allowing for proactive adjustments that can prevent deviations and enhance product quality.

The real-time application of NIR spectroscopy, when coupled with multivariate analysis techniques, warrants specific investigation and troubleshooting. This innovative approach could revolutionize process development activities by enabling continuous

monitoring, which conserves time and materials but also enhances the overall efficiency of the Stage 1 validation activities. Ultimately, such advancements have the potential to significantly accelerate the time to market of biopharmaceutical products, thereby improving patient access to essential therapies and fostering a more responsive and agile pharmaceutical industry.

In the present paper, an in-line application of NIR is documented to investigate the system's ability to identify possible fault detection occurring during a freeze-drying cycle. Moreover, the RM trend was evaluated to determine the endpoint of primary drying phase and compare it with the one calculated from the Pirani–Baratron method. NIR spectra were acquired in-line during freeze-drying runs. Firstly, an in-line statistical quality control system was developed based on multivariate control charts involving two statistics: Hotelling's T2 and the Distance to the Model (DModX). SIMCA software (Sartorius, version 18.0) was used for data analysis. Two batches obtained under Normal Operating Conditions (NOCs) were used to train a reference model of the process based on Principal Component Analysis (PCA). Different control limits were evaluated and set as reference and acceptable. Then, an additional cycle, intentionally simulating a failure during the process was projected into the developed space [27,28]. In the second part of the work, the residual moisture trend was evaluated in the three cases using an off-line developed Partial Least Squared Regression (PLS) model. The aim of this step was to assess the endpoint detection of the primary drying stage according to the trend of water content while the process is occurring. A comparison with the endpoint detected by the Pirani–Baratron method in the three cases was performed to assess the reliability of the PLS model.

2. Materials and Methods

2.1. Case Study and Sample Preparation

2.1.1. In-Line Measurement Set-Up

For the development of the statistical quality control model, 2R glass vials (Nuova Ompi, Piombino Dese, Italy) were filled with 1 mL of sucrose 5%$_w$ aqueous solution. Ultrapure water by a Millipore water system (IQ 7000, Merck Millipore, Burlington, VT, USA) was used for the preparation of the solution, while sucrose was supplied by Merck Life Science (Darmstadt, Germany).

Freeze-drying runs were carried out in a laboratory scale freeze-dryer (Lyostar 3, SP Scientific, Warminster, PA, USA) using the in-line NIR probe (Antaris MX FT-NIR, Thermo Fischer, Waltham, MA, USA) pointing out on a specific sample. Specifically, the chamber door of the freeze-dryer was provided by a special flange, designed ad hoc to allow the installation of a single NIR probe for in-line spectra acquisition, as shown in Figure 1a. In all tests, 23 vials were placed in a polymeric frame, whose side contained a carving shaped for probe positioning and keeping it in contact with the monitored sample (Figure 1b). Temperature control was performed by means of two thermocouples, while pressure monitoring was performed with a capacitance manometer and a Pirani sensor.

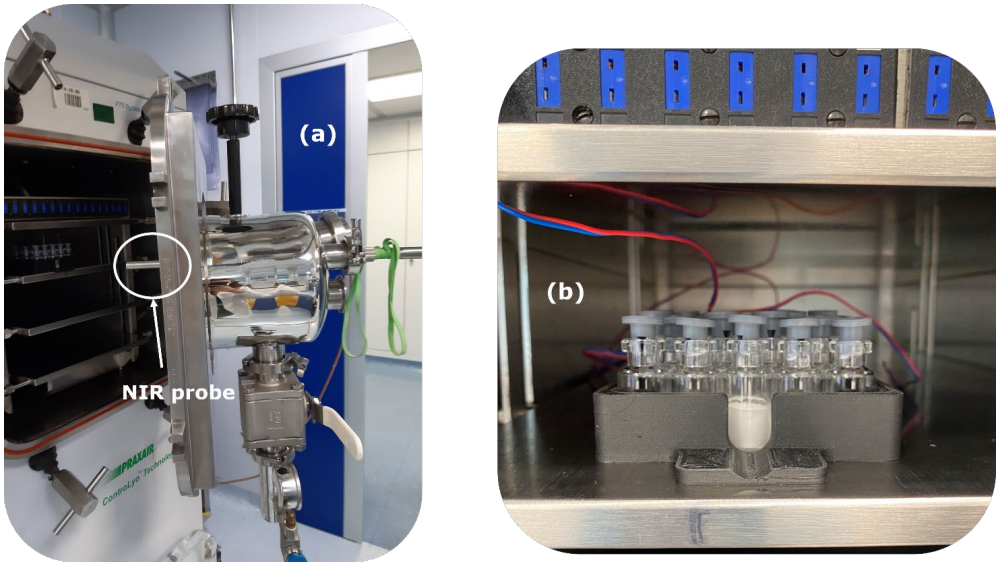

Figure 1. Set-up for in-line NIR spectroscopy in freeze-drying process. In figure (**a**), the installation of the NIR probe in the freeze-dryer chamber is shown, while in figure (**b**), the samples arrangement is shown.

The Normal Operating Conditions used for the reference freeze-drying cycles (named as "Cycle 1" and "Cycle 2") were the following:

- Freezing at −45 °C for 6 h (cooling/heating rate set at 2 °C/min)
- Primary drying at −25 °C and 5 Pa for 30 h
- Secondary drying at +35 °C and 5 Pa for 10 h

In the fault cycle, named as "Cycle 3", shelf temperature was decreased to −15 °C after 24 h of primary drying. Then, it was restored to −25 °C and held for 30 min. Afterwards, the chamber pressure was gradually increased to 10 Pa after another 30 min of primary drying and to 15 Pa after 20 min of primary drying. This cycle was used to prove the ability of the model to detect faults occurring during the process. In both cases, spectra were acquired in a continuous mode each 2 min for the entire duration of the lyophilization cycle.

2.1.2. Experiments for Quantification of Residual Moisture

For the quantification of the trend of residual moisture, a sucrose 6%$_w$ aqueous solution (labeled as S6) was prepared. Ultra-pure water by a Millipore water system (IQ 7000, Merck Millipore, Burlington, VT, USA) was used for the preparation of the solution, while sucrose was supplied by Merck Life Science (Darmstadt, Germany). This formulation was freeze-dried into 2R glass vial (Nuova Ompi, Piombino Dese, Italy) with a filling volume of 1 mL using the reference cycle described above. For the calibration of the PLS model, a wide range of moisture in the samples is needed. Therefore, a manual humidification was carried out to obtain a RM between 0 and 5% by adding a certain amount of water into the stopper and leaving the vials in upside position over-night, leading the evaporation and diffusion of water in the sample.

Then, the spectra were acquired off-line using a Fourier Transform NIR spectrometer (Antaris MX FT-NIR, Thermo Fischer Scientific, Waltham, CA, USA) equipped with an InGaAs detector and a halogen NIR source. The acquisition was performed in diffuse reflectance mode in the full wavelength range 10000–4000 cm^{-1}, averaging between 96 scans to obtain a single spectrum. After the acquisition of the spectra, Karl Fischer (KF) titration was performed on the samples to obtain the reference values of residual moisture. A coulometric titrator was employed (C30S Mettler Toledo, Columbus, OH, USA) for this

purpose. Formamide and methanol are the reactants required by Karl Fischer titration, and the water content percentage was subsequently calculated according to the SOP of the company.

2.2. Multivariate Data Analysis

Spectroscopic techniques, such as NIR spectroscopy, generates a huge amount of data. Therefore, multivariate data analysis is needed to extract useful information from the NIR spectra [29]. The NIR spectra were organized as a big data matrix structured as follows:

- Each row represents an observation at a specific data point, the absorbance value;
- Each column represents a variable that is each specific wavenumber.

In the present work, PCA was used for in-line statistical quality control, while a PLS model was developed to track the residual moisture content during the different phases of the freeze-drying process. Before being subjected to the specific model, all spectra underwent the Standard Normal Variate (SNV) preprocessing technique to remove the noise of measurements, highlighting the signals [30].

2.2.1. Principal Component Analysis

PCA is an unsupervised method allowing for identifying relationships among the samples in a dataset. It is a bilinear decomposition aimed at reducing large volumes of data into a smaller dataset of parameters referred to as principal components (PCs) [31].

Usually, a spectral dataset is collected in a matrix $\boldsymbol{X}$ with dimension IxJ, where I represents the number of observations and J the number of variables involved. The PCA model decomposes the data matrix as follows:

$$\boldsymbol{X} = \boldsymbol{T} \cdot \boldsymbol{V}^T + \boldsymbol{E} \quad (1)$$

The number of components of the developed model is denoted as *A*. The score matrix, $\boldsymbol{T}$, has dimension *IxA* and contains the projections of the original observations in the new PC space. Conversely, the loading matrix, $\boldsymbol{V}$, has dimension *AxJ* and explores the impact of each original variable on the PC space. The unexplained variance of the data is found on the error matrix denoted as $\boldsymbol{E}$. The decomposition is achieved in such a way to maximize the variance among the data [32].

SIMCA® software version 18 was used to develop the PCA models.

2.2.2. Additional Statistical Variables

Once the new space has been modeled, atypical observations may emerge that do not conform to the structure of the new reference system. This can happen when the reference system fails to account for specific features present in these observations [33]. Such outliers can be identified using multivariate control charts (MCCs), which are based on two statistics: Hotelling's T^2 and the Distance to the Model DMod. SIMCA® software was used to develop the models since it is in compliance with Good Manufacturing Practice (GMP) environments and accepted in the perspective of data integrity and quality assurance of the pharmaceutical field [34,35].

The Hotelling's T2 plot illustrates the distance from the origin in the score space for each designated observation. A substantial T2 value for a specific observation, i.e., a value significantly exceeding the critical limits, signifies that the observation is distant from the others within the specified range of components in the score space. Hence, this is likely to be an outlier. The Hotelling's T2 for observation I, based on A components, is as follows:

$$T_i^2 = \sum_{a=1}^{A} \frac{t_{i,a}^2}{s_{ta}^2} \quad (2)$$

where s_{ta}^2 represents the variance related to the *a-th* PC, and $t_{i,a}$ is the *a-th* score vector. To track the progression of new observations, the tolerance limits for the control charts are typically computed using tolerance intervals based on the mean value ±3 times the standard deviation, considering the 95% and 99% values as the confidence interval [36,37].

On the other hand, the *DModX* indicates the distance from the model plane at which the observation is situated. In other words, it indicates the residual standard deviation between the data and the PC model. When these residuals are large, this indicates an abnormal behavior in the process. Specifically, observations with a DMod larger than the critical calculated value (*DCrit*) are outliers. This indicates that these observations are different from the normal observations with respect to the correlation structure of the variables [38].

2.2.3. Partial Least Squares Regression

Contrary to PCA, the PLS relies on the maximization of the covariance between the input data matrix, $\boldsymbol{X}$, and the output vector of attributes, $\boldsymbol{Y}$. It also reduces the dimensionality of the dataset by exploiting the latent variables *N*.

Similar to PCA, it applies a linear decomposition of both factors, $\boldsymbol{X}$ and $\boldsymbol{Y}$, in the new reduced space. The difference lies on the decomposition of $\boldsymbol{Y}$:

$$\boldsymbol{Y} = \boldsymbol{U} \cdot \boldsymbol{Z}' + \boldsymbol{F} \quad (3)$$

As in the case of $\boldsymbol{X}$ decomposition, here $\boldsymbol{U}$ denotes the score matrix (*IxN)*, $\boldsymbol{Z}$ is the loadings matrix (*JxA)* and $\boldsymbol{F}$ is the residual one. The scores of $\boldsymbol{X}$ can be estimated thanks to the coefficients collected in the weight matrix denoted as $\boldsymbol{W}$. Since $\boldsymbol{W}$ and $\boldsymbol{Z}$ are orthonormal, the weights can be transformed in a new matrix, $\boldsymbol{W}^*$, as follows:

$$\boldsymbol{T} = \boldsymbol{XW}(\boldsymbol{V}'\boldsymbol{W})^{-1} = \boldsymbol{XW}^* \quad (4)$$

The PLS is finalized to the calculation of the regression matrix $\boldsymbol{B}$ (*IxK)* that is obtained by linear combination of the transformed weights and the loading matrix of $\boldsymbol{Y}$. Once the regression matrix is obtained, the attributes ($\boldsymbol{Y}_{\mathbf{pred}}$) of the new observation ($\boldsymbol{X}_{\mathbf{new}}$) can be calculated:

$$\boldsymbol{B} = \boldsymbol{W}^* \cdot \boldsymbol{Z}' \quad (5)$$

$$\boldsymbol{Y}_{\boldsymbol{pred}} = \boldsymbol{B} \cdot \boldsymbol{X}_{\boldsymbol{new}} \quad (6)$$

The performance of the model was evaluated by computing the root mean square error of calibration (RMSEC) and cross-validation (RMSECV). The RMSE serves as an indicator of the average prediction error, illustrating the variation between predicted and actual values, and can be determined using the following equation:

$$RMSEC = \sqrt{\frac{\sum_{i=1}^{M_{cal}} \left(y_i^{cal} - y_{pred,i}^{cal}\right)^2}{M^{cal}}} \quad (7)$$

M_{cal} represents the number of observations in the calibration set. Additionally, y_i^{cal} and $y_{pred,i}^{cal}$ denote the i-th sample from the training set, with values measured by traditional methods and predicted by the model. The averages of the observed values for the dependent variable in the calibration set is reported as $\overline{y^{cal}}$ [39].

2.3. Development of Models

2.3.1. Multivariate Control Charts

To develop the multivariate control charts, PCA was employed. Firstly, a PCA model including the reference runs was carried out to gain a deeper understanding of the freeze-drying cycles and see if any differences were highlighted. Then, the spectra belonging to the freezing stage were appropriately removed since NIR spectroscopy is sensitive only to the drying stages. A new PCA model was calibrated using the reference cycles in a wide range of wavenumber (7400–4230 cm^{-1}) focusing only on the spectra belonging to the drying phases. The corresponding control limits were evaluated and used to track in-line the behavior of a new cycle, intentionally causing a deviation from the normal behavior.

2.3.2. PLS Model for RM In-Line Estimation

Water exhibits prominent absorption bands, with peaks located at around 6800 cm^{-1} and 5150 cm^{-1}. A PLS model was calibrated in the range 7400–4230 cm^{-1} of wavenumber and in the range 0–5% of residual moisture. The model was constructed on SNV pretreated spectra with two latent variables. As a graphical outcome, parity plot relating the RM measured by KF as a function of RM predicted by the model is reported.

The PLS model was developed within a specific range of sucrose concentration. However, based on the findings of Massei et al. [17] and Bobba et al. [16], by focusing on the region where the water peak is located and, thus, is mostly affected by the residual moisture, this model could be generalized to encompass different formulations. Consequently, in this manner, the signals related to the specific product do not play a relevant role in the quantification of the residual moisture.

3. Results

3.1. Statistical Quality Control

3.1.1. A Deeper Understanding of the Freeze-Drying Cycle: PCA of In-Line Acquired NIR Spectra

All the spectra, related to the reference freeze-drying cycles, were subjected to SNV pretreatment and then were analyzed by a PCA over the range 7400–4230 cm^{-1}. Indeed, the behavior for higher or lower frequencies was found to be meaningless since the spectra appeared flat or too noisy. The first two PCs of the PCA model were found to be the most significative since they explained more than 97% of the variance among the spectra. After performing PCA with SIMCA software, two graphs named score plot and loading plot were obtained for each principal component investigated.

The spectra of an observation for each phase, randomly selected from the clusters obtained from the score plot, are shown in Figure 2 to gain a deeper understanding of the freeze-drying process. In graph (a), the spectrum associated to the freezing phase is shown, reporting a relatively stable baseline. The absorbance values do not exhibit significant peaks, indicating that NIR spectroscopy is less effective in this phase. This can be primarily attributed to the solidification of the formulation, which limits the interaction of the NIR light with the water molecules. As a result, the spectral information gained at different time instants from this phase is not useful for the aim of the analysis.

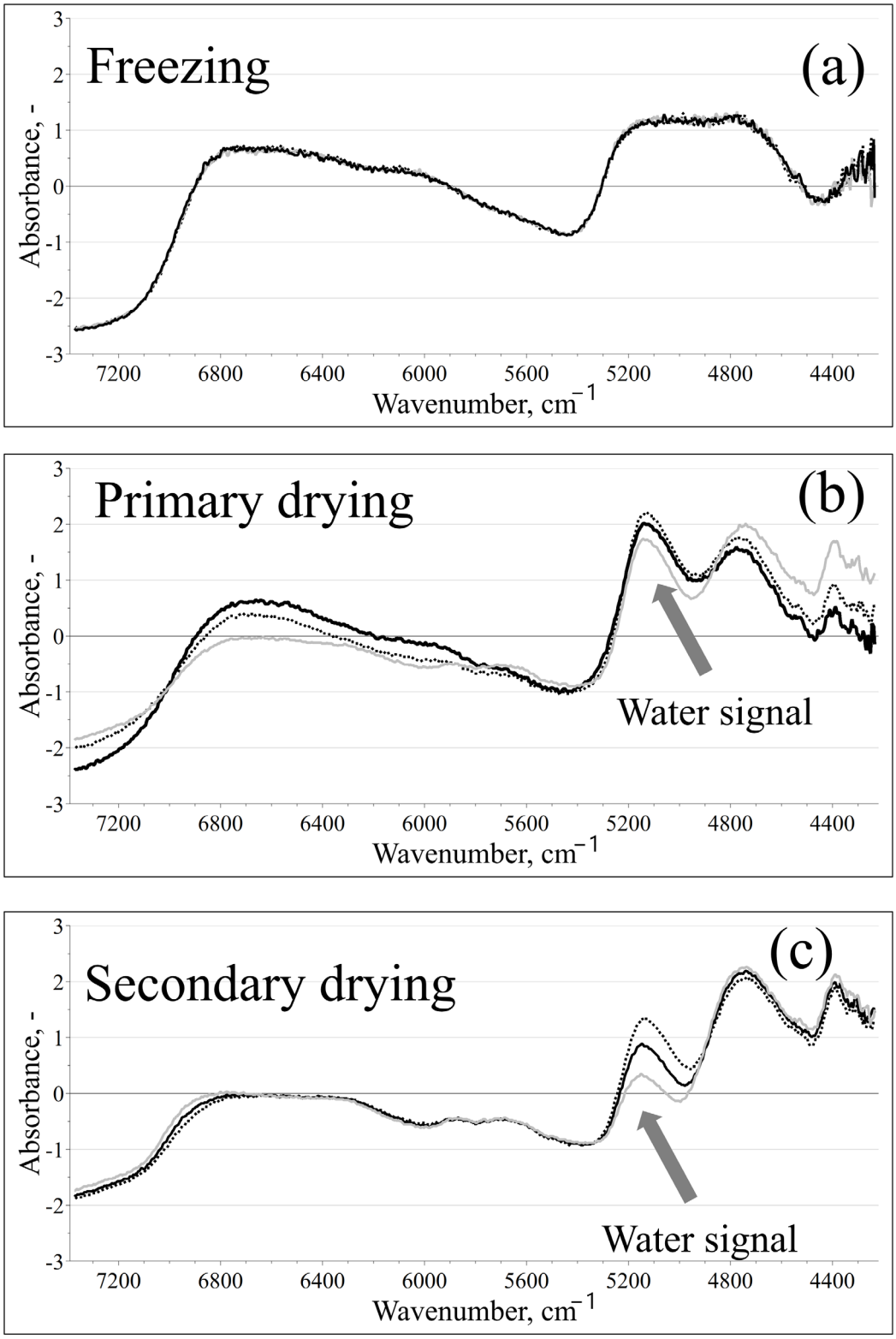

Figure 2. NIR spectra of a generic observation belonging to phase at different time instants: (**a**) freezing, (**b**) primary drying and (**c**) secondary drying. The signal of water is highlighted.

During the primary drying phase, as depicted in graph (b), a notable peak appears around 5200 cm^{-1}, corresponding to the water signal. This peak indicated the sublimation of ice and the transition of water from a solid to a vapor state. The absorbance value fluctuates significantly in this phase, reflecting the changes in moisture content as ice sublimates. The data collected during this phase allow for a better monitoring of the freeze-

drying process, providing insights into the physicochemical changes occurring in the formulation.

Lastly, during the secondary drying phase shown in graph (c), the spectrum shows the same peak at around 5200 cm^{-1} but at a lower intensity with respect to the primary drying phase. At a certain point, this signal stabilizes, indicating that most of the bound water has been removed and the formulation reached a stable state.

Initially, all spectra, regardless of the phase of the freeze-drying cycle, were analyzed using PCA. Figure 3 shows an example of score plot relating PC1 as a function of the PC2. The score plot illustrates the distribution of samples across the first two principal components obtained from the NIR spectra collected in-line during the freeze-drying process. Three different regions were highlighted in the graph according to the phase of the process. Indeed, in the freezing phase, samples cluster closely in a random way since NIR is not sensitive to this specific process step. As the process moves to primary drying, the scores shift because of changes in the material's properties due to ice sublimation. As the primary drying phase progresses, ice disappears, due to sublimation, and then also the residual moisture in the dried product, i.e., the water remained entrapped in the solid matrix in the freezing stage (the "bound water"), decreases. NIR spectroscopy is able to detect this change as we observe a decrease in scores along PC2 and an increase along PC1. As the process moves into the secondary drying phase, the scores begin to increase in both PC1 and PC2. What emerges in this step is a stabilization along PC1, suggesting that the overall composition and structure of the formulation are becoming more consistent. In fact, as the drying process concludes, the values along PC1 stabilize, indicating the stabilization of the spectrum and, therefore, smaller changes in the active pharmaceutical ingredient's (API) and excipients' composition. The differences observed in the score plot can be related to the difference in process variables, as depicted in Figure S1 in the Supplementary Materials. In Figure S1a, the shelf temperature, the product temperature and the condenser temperature profiles are reported. The trend of the variables highlighted the correct behavior occurred during the freeze-drying cycle during the three different phases (freezing, primary drying and secondary drying). Figure S1b illustrates the pressure profiles and the alignment between the Pirani and Baratron sensors for both cycles. As expected, the alignment of Pirani and Baratron sensor is quite equal for the two cycles performed under the same operating conditions.

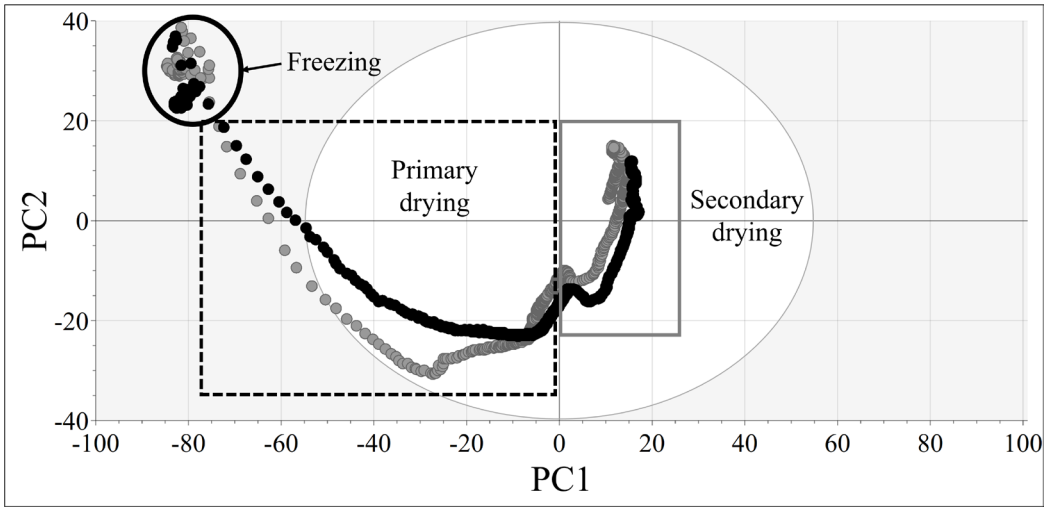

Figure 3. Score plot relating the first two principal components of the NIR spectra acquired in-line during the freeze-drying process. Data were processed by PCA in the range 7400–4230 cm^{-1}. The data are colored in black or grey for reference cycles 1 and 2, respectively.

This trend is confirmed by the behavior of the loading plot, reported in Figure S2 in the Supplementary Materials. In fact, they provided the contributions of specific wavenumbers to the principal components and provided valuable insights into the moisture dynamics. Specifically, the peak around 5200 cm^{-1} is related to free water and is significant in the loadings of PC2 as denoted in graph (b). In fact, a positive correlation is found since the peak is negative in the loading plot: a decrease in PC2 scores suggests that the removal of free water is a significant factor during the primary drying phase. This is also confirmed by the same peak noticed in the loadings of PC1 (graph a).

3.1.2. Process Control: How to Monitor Possible Faults Occurring during Freeze-Drying Cycles

As reported in the Introduction Section, in the context of process control within the pharmaceutical industry, the use of robust methods is essential for ensuring product quality. To achieve this, two reference freeze-drying cycles were employed to develop a PCA model, which serves as a reference for the monitoring of the process. The calculation of control limits based on Hotelling's T2 and DmodX was conducted using SIMCA software for comprehensive data analysis.

Given that NIR spectroscopy does not provide significant insights during the freezing phase, as demonstrated in Section 3.1.1, spectra obtained from this stage were excluded for the present analysis. Instead, the focus was directed towards the primary and secondary drying phases. The model was developed on the wavenumber range 7400–4230 cm^{-1}. The score plot of the new model is reported in Figure S3 in the Supplementary Information and confirmed what was previously discussed in Section 3.1.1. No changes in the behavior of the score plot were observed when the freezing stage was removed from the dataset.

Figure 4 depicts two key plots related to the analysis of two reference freeze-drying processes. The first cycle is reported in black, and the second one, run under the same operating conditions, is denoted in grey for the sake of clarity. The use of both Hotelling's T2 and DmodX weighted residuals help in monitoring each process and identifying deviations from expected behavior.

Figure 4a,b show the Hotelling's T2 statistics over the observations for both processes. The black and grey dashed lines indicate the critical values for T2 at 95% and 99% confidence levels, respectively. Values exceeding these limits suggest that the observations are outside the expected variability of the system. For both processes, the initial observations show high T2 values. This could be consistent with the early stages of primary drying where rapid sublimation occurs, leading to rapid changes in the system's dynamics, which can cause significant variations in the measured parameters. In fact, in the starting instants of primary drying, temperature and pressure conditions can fluctuate significantly as the ice transitions to vapor. Therefore, these initial points above the limits can be attributed to the period in which the material is adjusting to the new conditions, and the sensor is monitoring a mixture of frozen and (partially) dried material. After the initial phase, T2 values for both processes drop below the 95% control limit, indicating that the processes stabilize.

The plot in Figure 4c,d displays the DModX weighted residuals for both processes, measuring how far each observation deviates from the model predictions. This can be useful also to identify potential outliers in the data. The dashed line represents the critical limit. Observations exceeding this limit are considered statistically significant deviations from the expected model. Similar to the T2 plot, the DModX values for both processes are initially high, reflecting non-equilibrium conditions during the early drying phase. This aligns with the earlier explanation regarding the instability of the system. After the initial phase, the DModX values stabilize for both processes, indicating that they have reached a

more consistent state. Some outlier observations were identified at around observation 550 and were critically analyzed by looking into detail at their NIR spectra (reported in Figure S4 in the Supplementary Materials). Some anomalies in the data collection process occurred during the acquisition, arising maybe from instrumental noise of measurement or external disturbances. External disturbances or measurement noise can arise from various factors, including environmental fluctuations in temperature, humidity and pressure, as well as mechanical vibrations of the freeze-dryer or incorrect calibration of the NIR equipment. While it is challenging to control the underlying causes of disturbances, it is essential to ensure that the NIR instrumentation is consistently calibrated and properly maintained. However, it is important to remove potential outlier acquisition from the dataset to properly analyze data.

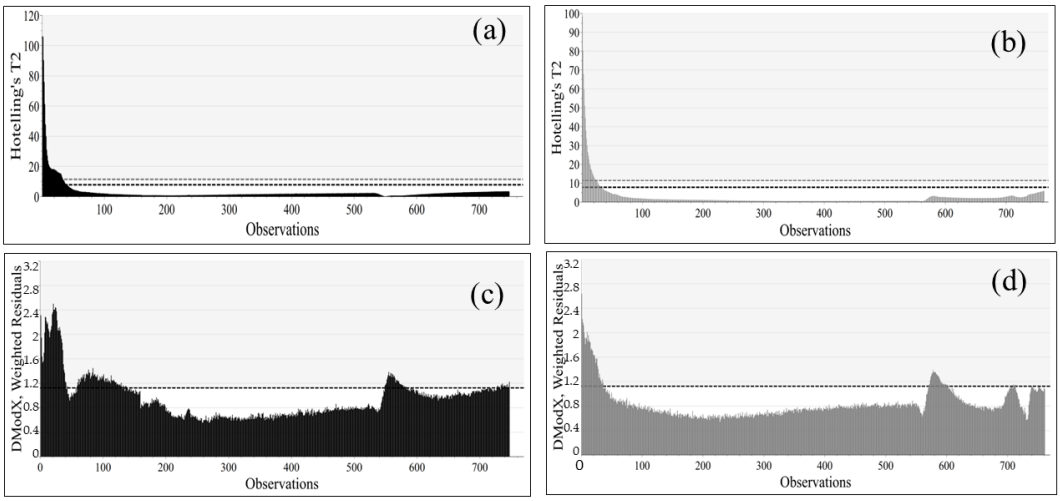

Figure 4. Hotelling's T2 plot (**a**,**b**) and DModX weighted residual plot (**c**,**d**) as a function of observations in the case of reference cycles. In black, reference cycle 1 is reported (**a**,**c**), while in grey, reference cycle 2 (**b**,**d**).

After having assessed this PCA model, the cycle intentionally conducted under fault conditions was projected into the existing space. By introducing these fault conditions, we aimed to challenge the robustness of the model and verify its sensitivity to variations that may indicate potential issues in the lyophilization process. The results from this projection are reported in Figure 5.

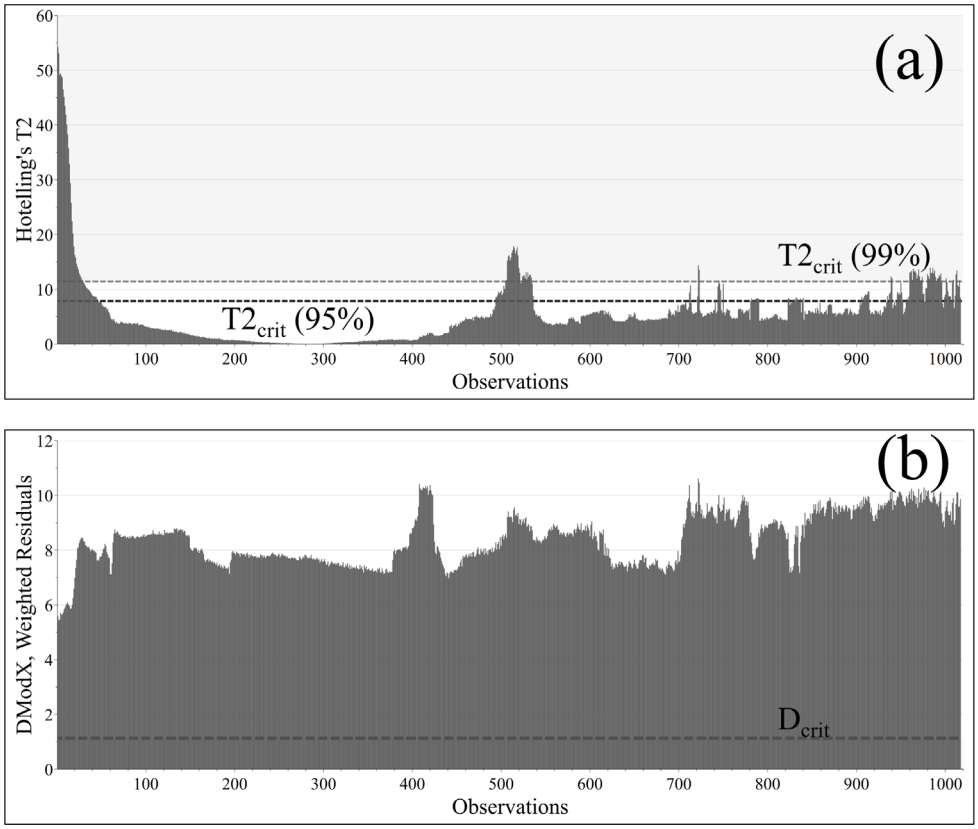

Figure 5. Hotelling's T2 plot (**a**) and DModX weighted residual plot (**b**) as a function of observations in the case of fault cycle.

In the Hotelling's T2 plot, reported in Figure 5a, it is possible to notice some observations exceeding the critical limits. This is perfectly reasonable since at a time instant, corresponding to the 500 observations, the shelf temperature was increased from −25 °C to −15 °C. Therefore, the T2 plot is able to identify the deviation from the expected process behavior. After around one hour, the process operating conditions were reported at the target ones, and this can be also reflected in the graph 5a since the subsequent points are below the critical limits calculated. However, a gradual pressure increase performed in the next time points is also detected by this chart since other points exceeding the critical limits were noticed.

In contrast to the T2 plot, nearly all observations in the DModX plot exceed the critical limit as shown in Figure 5b. This indicates that the model identifies a consistent level of deviations across the entire cycle, suggesting that the fault conditions significantly impacted the overall process dynamics. While the Hotelling's T2 can detect specific points of deviation from the mean within the model, the DModX metric is more sensitive to cumulative deviations throughout the cycle. This demonstrates the complementary nature of these metrics in monitoring the lyophilization process, with T2 providing insights into specific anomalies and DModX capturing broader, cumulative deviations. The reduced effectiveness of T2 control charts in monitoring batch processes has been previously documented in the literature, primarily attributed to the significant autocorrelation present in the data [10].

However, this approach may prove to be advantageous when a substantial number of variables are available, thereby allowing it to be regarded as an in-line application. Consequently, the next step would involve the application of a prediction algorithm to facilitate in-line monitoring without the necessity of waiting for the completion of the

cycles. It is important to note that the primary differences are observed at the onset of the cycle; therefore, the considerations presented herein are deemed reliable.

3.2. Evolution of RM Using In-Line Monitoring

When the instant values of T2 and DModX are below the threshold, a quantitative analysis could be gained. To reach this aim, a PLS model was developed by considering the entire dataset deeply explored in previous works by Bobba et al. and Massei et al. [16,17]. In this stage, all datasets were used to calibrate the model and the comparison between the RMSEC, and the RMSECV was conducted to assess the model's performances. This comparison serves as important metrics for understanding how well the model fits the training data versus its ability to generalize to unseen data.

Figure 6 presents the parity diagram plot comparing the residual moisture measured by KF against the RM values predicted by the PLS model. Each point in the graph corresponds to an observation. The proximity of the data points to the bisector (dashed line) indicates that the model is effectively capturing the relationship between the two variables. The alignment suggests that the model's predictions are reliable and consistent with the actual measurements, reflecting model accuracy in estimating the response variable.

The choice for developing the model in a wider range of residual moisture values arises from the intrinsic heterogeneity of the freeze-drying process, as well as the vial placement in the freeze-dryer. Indeed, the position of the vials within the freeze-dryer can affect how uniformly they are subjected to temperature and pressure changes during the process. Vials placed closer to the walls of the freeze-dryer may experience different thermal conditions compared to those positioned in the center. For instance, vials on the edges may be exposed to higher heat transfer rates, leading to faster sublimation and potentially lower residual moisture. Conversely, vials located in the center may dry more slowly due to lower amount of heat received, resulting in higher moisture retention. Moreover, variations in the freeze-drying environment, such as temperature gradients and pressure fluctuations, can affect the sublimation rate of the vials.

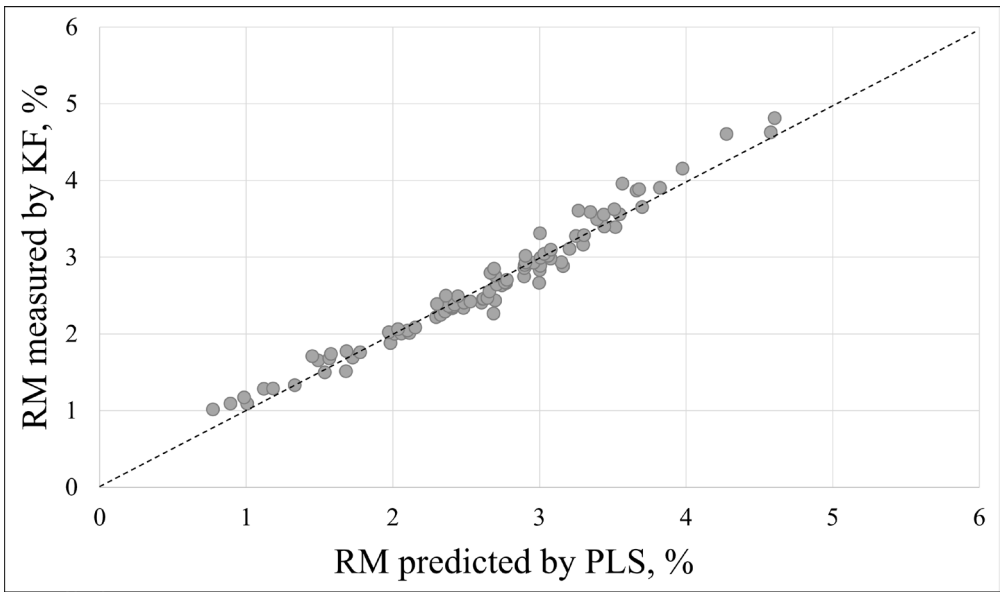

Figure 6. Parity diagram plot relating the measured RM values by KF as a function of the RM predicted by PLS model.

The model demonstrates a strong fit to the calibration data, as evidenced by the low RMSEC equal to 0.152%. Also, good predictive performances are evaluated, with a RMSECV equal to 0.156% when applied to unseen data during cross-validation. The

proximity of RMSEC and RMSECV values suggests that the model is not overfitting. This is a positive outcome as it implies that the model can generalize well to new observations, maintaining its accuracy without being overly tailored to the specific calibration dataset.

At this stage, the in-line acquired NIR spectra were input into the presented PLS model to calculate the evolution of residual moisture throughout the cycle and to assess the endpoint of the primary drying step. A comparison with the estimated drying time from the ratio between Pirani and Baratron profiles was conducted for validating the results, as reported in Figure 7.

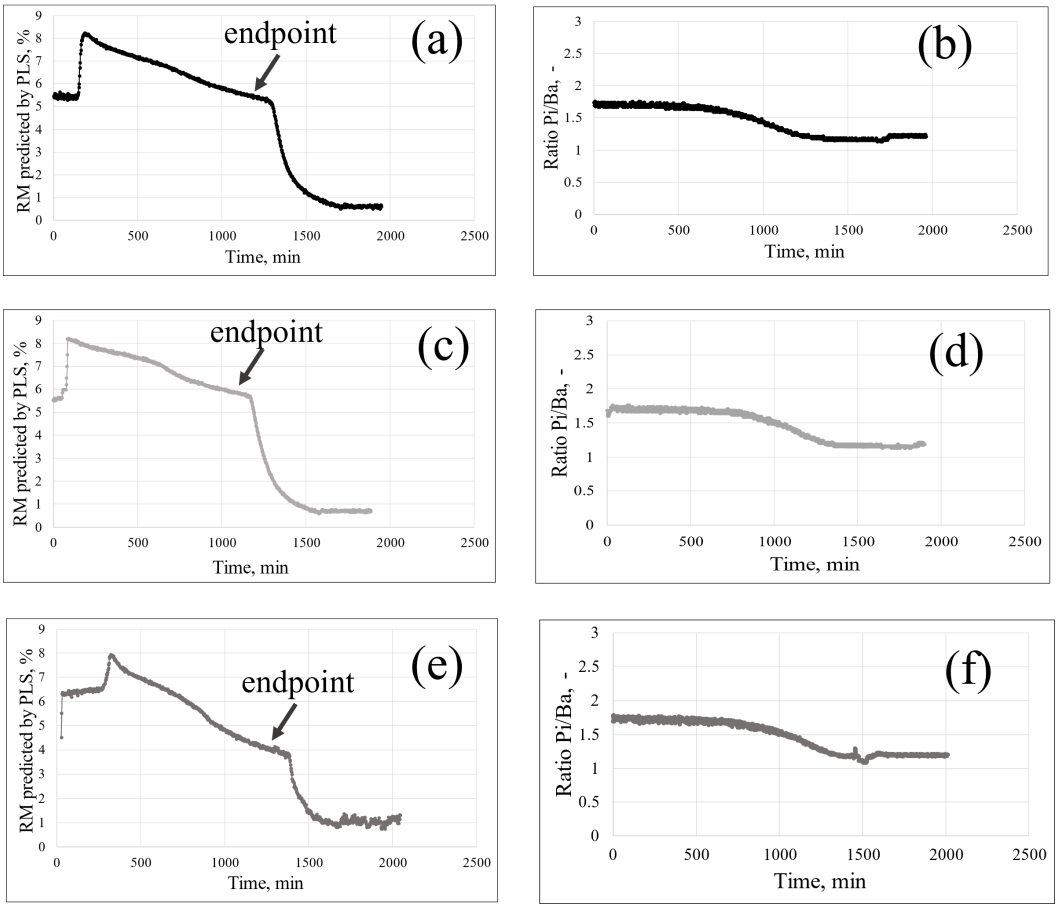

Figure 7. Graphs (**a**,**c**,**e**) depict the trend of residual moisture predicted by PLS model as a function of drying time in case of reference cycle 1, reference cycle 2 and fault cycle, respectively. In the graphs (**b**,**d**,**f**), the corresponding Pirani/Baratron ratio for the three cases is reported.

Figure 7a,c,e depict the predicted residual moisture values over time during the primary and secondary drying cycles. Specifically, the data analyzed from the two reference cycles and from the fault cycle are reported. In the three graphs, there is a noticeable decline in RM during the initial stages, indicating effective moisture removal. The steep drop in moisture levels suggests that the primary drying is efficiently progressing. The endpoint of the primary drying phase was marked in all graphs, signifying the transition to the secondary drying phase. Following the endpoint, the graphs show an additional decrease in RM. The residual moisture trends stabilize towards the end of the drying process, indicating that the target moisture content has been achieved in both cases. Moreover, similar asymptotic values were found: RM was equal to 0.60% for the first reference cycle and equal to 0.68% for the second reference cycle. This was expected since the two cycles were conducted in the same operating conditions.

Figure 7b,d,f illustrate the ratios of pressure measurements between the Pirani and Baratron sensors over time. These graphs are helpful to assess the endpoint of the primary drying step aiming to have a comparison with the value predicted by the PLS model. In both curves, the initial value is approximately 1.7 as the Pirani sensor measurements are based on the thermal conductivity of the gas within the drying chamber, resulting in readings that are about 60% higher than those from Baratron manometer. When the gas composition shifts from water vapor to nitrogen, the ratio Pitani/Baratron starts to decline, indicating the sublimation is occurring. The point at which this decrease starts is denoted as "onset", while the point where the lower asymptote is reached is the known as the "offset". Research has indicated that the onset, offset and midpoint can serve as indicators of drying time [40]. In the present work, the endpoint has been identified from the Pirani/Baratron ratio by considering the onset as criteria. As explained by Patel et al. [40], the moment at which the ratio begins to significantly decline (i.e., the onset) signifies a transition in gas composition from water vapor to nitrogen. This indicates that the sublimation can be considered completed in most of the batch.

Table 1 compares the endpoints calculated using two different methods: PLS and the Pirani–Baratron ratio.

Table 1. Comparison of endpoint estimated by PLS model and Pirani/Baratron ratio for the reference cycles and fault one. The relative error is also reported.

	Endpoint by PLS, h	Endpoint by Pi_Ba, h	Relative Error, %
Cycle 1	21	22	4.55
Cycle 2	19	21	9.52
Cycle 3	22	23	4.35

The endpoints derived from both methods for each cycle are close, indicating that the PLS approach yields consistent results. Notably, the PLS method tends to estimate slightly lower endpoint values compared to the Pirani/Baratron ratio across all cycles. The close alignment of the endpoint values reinforces the validity of PLS model for monitoring the lyophilization process. The relative error is also reported for the three cases, leading to optimal results with values always lower than 10%. This is entirely justified as it is essential to note that the values of drying times are influenced by a significant degree of uncertainty, given that they are determined through graphical methods. Also, a small portion of the error could be attributed to the fact that the PLS model is developed on a different percentage of sucrose in aqueous formulation. In any case, it has to be highlighted that, for industrial applications, a relative error lower than 10% is considered acceptable for process development activities. It has to be noted that although an edge vial is monitored by NIR, i.e., a vial whose drying time is considerably lower than that of the rest of the batch, the endpoint detected for this vial appears to be quite close to that detected through the well-established pressure-ratio-based method, thus making the method suitable for detecting the endpoint of the whole batch, although a non-central vial is monitored. This may be due to the setup proposed in this paper, shown in Figure 1, where the monitored vial appears to be quite shielded from radiation from chamber walls.

4. Strength and Weakness of the Proposed Methods

- The proposed methods utilizing Near-Infrared (NIR) spectroscopy for the real-time monitoring of the freeze-drying process in the biopharmaceutical industry presents several strengths and weaknesses that have to be properly accounted for in order to adequately apply them in the process development stage.
- As it is well known, NIR spectroscopy allows for non-destructive, real-time measurements, highly sensitive to moisture. Therefore, the use of NIR spectroscopy aligns

with the principles of Process Analytical Technology (PAT), which emphasizes the need for real-time data to enhance process understanding and control. Moreover, by continuously monitoring critical parameters such as residual moisture content, NIR spectroscopy enables timely interventions that can prevent batch failures. Additionally, other pros have been pointed out in this study:

- NIR spectra acquired in a reference cycle may be used to develop a PCA model, and, finally, multivariate control charts, utilizing Hotelling's T^2 and DModX metrics, may be obtained. They may effectively be used to identify process deviation from reference conditions.
- NIR spectra may be integrated with the Partial Least Squares (PLS) regression algorithm to adequately estimate the endpoint of the primary drying step.
- Both issues are highly appreciated in pharma R&D departments where they allow a speeding up of the DP process development phases and optimize the overall freeze-drying process. In fact, having a tool capable of detecting the primary drying endpoint with a very low error (below 10%) and identifying potential faults during the freeze-drying cycle, for the tested operating conditions, would facilitate time and resource savings in the development of the lyophilization process. More broadly, it would also expedite Stage 1 validation activities. On the other side, the weaknesses of the proposed methods have to be taken into account:
- One drawback is related to the fact that the system is based on a single vial monitoring, while it is well known that a batch of vials may be highly heterogeneous and, in particular, the edge vials experience a different thermal history with respect to the central ones. With this respect, it has to be highlighted that the monitored vial is the one subjected to the highest heat exchange as it is exposed to the freeze-dryer wall. Consequently, it is the first to experience the consequence of a change in process conditions. This characteristic facilitates the prompt recognition of any potential failures. In contrast, for endpoint monitoring, the edge vial is the first to complete the sublimation process. However, in the setup proposed in this paper, shown in Figure 1, the monitored vial appears to be quite shielded from radiation from chamber walls, and the endpoint detected for this vial appears to be quite close to that detected through the well-established pressure-ratio-based method, thus making the method suitable for detecting the endpoint of the whole batch, although a non-central vial is monitored.
- Integration in manufacturing facilities may be quite challenging. This reluctance stems from various factors, including the need for regulatory compliance, the complexity of implementing new technologies, and the necessity for staff training to ensure the proper usage and interpretation of the data. As the pharmaceutical industry continues to evolve towards a more data-centric approach, it is essential to advocate for the adoption of these innovative techniques in manufacturing environments as well. Obviously, the use of this system at lab scale, for process development purposes, does not pose any of these issues.
- Multiple and diverse fault conditions should be tested to point out the robustness of the present approach. In any case, we do not expect any different behavior in case multiple faults affect the residual moisture of the product vs. time as the method is based on the in-line detection of the residual moisture, and the fault is detected in case this parameter is not as expected, whatever the cause of this variation.

5. Conclusions

The current study highlights the successful application of NIR spectroscopy for the real-time monitoring of the freeze-drying process, emphasizing its potential for enhancing process understanding and control. The presented approach aligns with the increasing emphasis on Process Analytical Technology (PAT) in the perspective of a Quality by Design framework.

By concentrating on the drying phases, we can leverage the capabilities of NIR spectroscopy to gain valuable insights into the physiochemical changes occurring within the formulation. Moreover, we can also detect in real-time possible faults occurring during a freeze-drying cycle, avoiding the impairment of the entire batch. In fact, the ability to identify deviations from expected behavior using Hotelling's T2 and DModX metrics provides an effective means of maintaining product quality throughout the freeze-drying process.

The application here reported requires the ending of the freeze-drying cycle or could be applied with a safety margin if most of the variation occurs at the beginning of the cycle itself. Therefore, a prediction algorithm could facilitate the in-line monitoring of freeze-drying without waiting for the ending of the cycle. Another important remark is related to the fact that NIR spectroscopy is particularly sensitive to residual moisture in the dried product; thus, inaccurate evaluations may be obtained in the first part of the primary drying stage where a mixture of frozen and (partially) dried product is monitored.

Moreover, the results demonstrated that the endpoints calculated using both PLS and Pirani–Baratron methods were closely aligned, indicating the reliability of the PLS model in predicting moisture levels and to track in-line the evolution of the drying phases. The low relative errors observed further reinforce the model's robustness, making it a valuable tool for process control.

Supplementary Materials: The following supporting information can be downloaded at www.mdpi.com/xxx/s1. Figure S1: Process variables for the reference cycles; graph (a): Temperature profiles and (b) Pressure profiles; Figure S2: Loading plot relating the first principal component (a) and the second one (b) as a function of the wavenumber. Data were processed by PCA in the range 7400–4230 cm^{-1}; Figure S3: Score plot relating the first two principal components of the NIR spectra acquired in-line during the freeze-drying process by considering only the drying stages. Data were processed by PCA in the range 7400–4230 cm^{-1}. The data are colored, respectively, in black or grey for reference cycles 1 and 2; Figure S4: NIR spectra investigation of the anomalous sample noticed in the Hotelling's T2 plot for reference cycle 1.

Author Contributions: Conceptualization, D. F.; formal analysis, A.M.; investigation, A.M.; project administration, N.F.; resources, N.F.; software, A.M.; supervision, N.F. and D.F.; writing—original draft, A.M.; writing—review and editing, A.M., N.F. and D.F. All authors have read and agreed to the published version of the manuscript.

Funding: The research project was founded by Merck Serono.

Data Availability Statement: The original contributions presented in this study are included in the article/Supplementary Materials. Further inquiries can be directed to the corresponding author. The raw data supporting the conclusions of this article will be made available by the authors on request.

Conflicts of Interest: Authors Ambra Massei and Nunzia Falco were employed by the Merck Serono. The remaining authors declare that the research was conducted in the absence of any commercial or financial relationships that could be construed as a potential conflict of interest. The Merck Serono had no role in the design of the study; in the collection, analyses, or interpretation of data; in the writing of the manuscript, or in the decision to publish the results.

References

1. van Sprang, E.N.M.; Ramaker, H.; Westerhuis, J.; Gurden, S.; Smilde, A. Critical evaluation of approaches for on-line batch process monitoring. *Chem. Eng. Sci.* **2002**, *57*, 3979–3991.
2. Deloitte. Measuring the Return from Pharmaceutical Innovation—14th Edition. 2023. Available: https://www.deloitte.com/uk/en/Industries/life-sciences-health-care/research/measuring-return-from-pharmaceutical-innovation.html (accessed on 1 October 2024).
3. Food and Drug Administration. Pharmaceutical cGMP for the 21st Century—A Risk-Based Approach. 2002. Available online: https://www.pharmaceuticalonline.com/doc/pharmaceutical-cgmps-for-the-21st-century-a-r-0001 (accessed on September 2004).
4. Lawrence, X.; Amidon, G.; Khan, M.; Hoag, S.; Polli, J.; Raju, G.; Woodcock, J. Understanding Pharmaceutical Quality by Design. *Am. Assoc. Pharm. Sci.* **2014**, *16*, 771–783.
5. Pramod, K.; Tahir, M.; Charoo, N.; Ansari, S.; Ali, J. Pharmaceutical product development: A quality by design approach. *Int. J. Pharm. Investig.* **2016**, *6*, 129–138.
6. Food and Drug Administration. PAT—A Framework for Innovative Pharmaceutical Development, Manufacturing, and Quality Assurance. 2004. Available online: https://www.fda.gov/regulatory-information/search-fda-guidance-documents/pat-framework-innovative-pharmaceutical-development-manufacturing-and-quality-assurance (accessed on 1 October 2024).
7. Fissore, D. Freeze-drying of pharmaceuticals. In *Encyclopedia of Pharmaceutical Science and Technology*; J. Swarbrick: London, UK, 2013; pp. 1723–1737.
8. Rambhatla, S.; Pikal, M. Heat and mass transfer scale-up issues during freeze-drying, I: Atypical radiation and the edge vial effect. *AAPS PharmSciTech* **2003**, *4*, 22–31.
9. Rambhtala, S.; Tchessalov, S.; Pikal, M. Heat and mass transfer scale-up issues during freeze-drying, III: Control and characterization of dryer differences via operational qualification tests. *AAPS PharmSciTech* **2006**, *7*, E61–E70.
10. Colucci, D.; Prats-Montalban, J.; Ferrer, A.; Fissore, D. On-line product quality and process failure monitoring in freeze-drying of pharmaceutical products. *Dry. Technol.* **2021**, *39*, 134–147.
11. Colucci, D.; Prats-Montalban, J.; Fissore, D.; Ferrer, A. Application of multivariate image analysis for on-line monitoring of a freeze-drying process for pharmaceutical products in vials. *Chemom. Intell. Lab. Syst.* **2019**, *187*, 19–27.
12. Blanco, M.; Coello, J.; Iturriga, H.; Maspoch, S.; de la Pezula, C. Near-infrared spectroscopy in the pharmaceutical industry. *Analyst* **1998**, *123*, 135R–150R.
13. Bobba, S.; Zinfollino, N.; Fissore, D. Application of Near-Infrared Spectroscopy to statistical control in freeze-drying processes. *Eur. J. Pharm. Biopharm.* **2021**, *168*, 26–37.
14. Lakeh, M.; Karimvand, S.; Khoshayand, M.; Abdollahi, H. Analysis of residual moisture in a freeze-dried sample drug using a multivariate fitting regression model. *Microchem. J.* **2020**, *107*, 2411–2502.
15. Clavaud, M.; Lema-Martinez, C.; Roggo, Y.; Bigalke, M.; Guillemain, A.; Hubert, P.; Ziemons, E.; Allmendinger, A. Near-infrared spectroscopy to determine residual moisture in freeze-dried products: Model generation by statistical design of experiments. *J. Pharm. Sci.* **2020**, *109*, 719–729.
16. Bobba, S.; Zinfollino, N.; Fissore, D. Evaluation of the Robustness of a Novel NIR-based Technique to Measure the Residual Moisture in Freeze-dried Products. *J. Pharm. Sci.* **2022**, *111*, 1437–1450.
17. Massei, A.; Falco, N.; Fissore, D. Use of machine learning tools and NIR spectra to estimate residual moisture in freeze-dried products. *Spectrochim. Acta Part A Mol. Biomol. Spectrosc.* **2023**, *293*, 122485.
18. Jones, J.; Last, I.; MacDonald, B.; Prebble, K. Development and transferability of near-infrared methods for determination of moisture in a freeze-dried injection product. *J. Pharm. Biomed. Anal.* **1993**, *11*, 1227–1231.
19. Grohganz, H.; Gildemyn, D.; Skibsted, E.; Flink, J.; Rantanen, J. Towards a robust water content determination of freeze-dried samples by near-infrared spectroscopy. *Analytica Chimica Acta* **2010**, *676*, 34–40.
20. Clavaud, M.; Roggo, Y.; Degardin, K.; Sacrè, P.; Hubert, P.; Ziemons, E. Global regression model for moisture content determination using near-infrared spectroscopy. *Eur. J. Pharm. Biopharm.* **2017**, *119*, 343–352.
21. Miller, P.; Swanson, R.; Heckler, C. Contribution plots: A missing link in multivariate quality control. *Appl. Math. Comput. Sci.* **1998**, *8*, 775–792.
22. Kirdar, A.; Conner, J.; Baclaski, J.; Rathore, A. Application of multivariate analysis toward biotech processes: Case study of a cell-culture unit operation. *Biotechnol. Prog.* **2007**, *23*, 61–67.
23. Garcia-Munoz, S.; Settell, D. Application of multivariate latent variable modeling to pilot-scale spray drying monitoring and fault detection: Monitoring with fundamental knowledge. *Comput. Chem. Eng.* **2009**, *33*, 2106–2110.

24. Kona, R.; Qu, H.; Mattes, R.; Jancsik, B. Application of in-line near infrared spectroscopy and multivariate batch modeling for process monitoring in fluid bed granulation. *Int. J. Pharm.* **2013**, *452*, 63–72.
25. De Beer, T.; Vercruysse, P.; Burggraeve, A.; Quinten, T.; Ouyang, J.; Zhang, X.; Vervaet, C.; Remon, J.; Baeyens, W. In-Line and Real-Time Process Monitoring of a Freeze Drying Process Using Raman and NIR Spectroscopy as Complementary Process Analytical Technology (PAT) Tools. *J. Pharm. Sci.* **2009**, *98*, 3430–3446.
26. Rosas, J.; de Waard, H.; De Beer, T.; Vervaet, C.; Remon, J.; Hinrichs, W.; Frijlink, H.; Blanco, M. NIR spectroscopy for the in-line monitoring of a multicomponent formulation during the entire freeze-drying process. *J. Pharm. Biomed. Anal.* **2014**, *97*, 39–46.
27. Mahar, P.; Verma, A. Pharmaceutical process validation: An overview. *Int. J. Pharm. Res. Bio-Sci.* **2014**, *3*, 243–262.
28. Dobbins, J.; Pluschkell, S.; Krause, P.; O'Neil, J.; Swann, P.; Welch, J. CMC forum: Evolution of biopharmaceutical control strategy through continued process verification. *BioProcess Int.* **2017**, *15*, 17–23.
29. Rajalahti, T.; Kvalheim, O. Multivariate data analysis in pharmaceutics: A tutorial review. *Int. J. Pharm.* **2011**, *417*, 280–290.
30. Rinnan, A.; Norgaard, L.; van den Berg, F.; Thygesen, J.; Bro, R.; Enelsen, S. Data Pre-Processing. In *Infrared Spectroscopy for Food Quality Analysis and Control*; Elsevier, Inc.: Amsterdam, The Netherlands, 2009; pp. 29–50.
31. MacGregor, J.; Kourti, T. Statistical Process Control of Multivariate Processes. *Control Eng. Pract.* **1995**, *3*, 403–414.
32. Massart, D.; Vandeginste, B.; Buydens, L.; Lewi, P.; Smeyers-Verbeke, K.; De Long, S. *Handbook of Chemometrics and Qualimetrics*; Elsevier Science Inc.: Alpharetta, GA, USA, 1998.
33. Torres, A.; de Oliveira, A.; Junior, S.; Fragoso, W. Multivariate statistical process control in annual pharmaceutical product review. *J. Process Control* **2018**, *69*, 97–102.
34. Sartorius. SIMCA® 17 Improves Spectroscopy Modeling for PAT and Supports Data-Driven Decision-Making. 09 February 2021. Available online: https://www.sartorius.com/en/knowledge/science-snippets/simca-17-improves-spectroscopy-modeling-for-pat-and-supports-data-driven-decision-making-671850?srsltid=AfmBOoosTyMNP1qV70YkzGKQ4rKjKqiqP-b_Fp_4F2ESCStRxiG5zwky (accessed on 1 October 2024).
35. Kresta, J.; MacGregor, J.; Marlin, T. Multivariate statistical monitoring of process operating performances. *Can. J. Chem. Eng.* **1991**, *69*, 35–47.
36. Albon, C. *Machine Learning with Python, Cookbook*; O'Reilly Media Inc.: Sebastopol, CA, USA, 2018.
37. Geron, A. *Hands-on Machine Learning with Scikit-Learn, Keras & TensorFlow—Concepts, Tools and Techniques to Build Intelligent System*; O'Reilly Inc.: Sebastopol, CA, USA, 2019.
38. SIMCA Sartorius. SIMCA 15 User Guide. 2020. Available online: https://www.sartorius.com/download/544940/simca-15-user-guide-en-b-00076-sartorius-data.pdf (accessed on 1 October 2024).
39. Amigo, J. Data Mining, Machine Learning, Deep Learning, Chemometrics. Definitions, common points and Trends. *Braz. J. Anal. Chem.* **2021**, *8*, 22–38.
40. Patel, S.; Doen, T.; Pikal, J. Determination of end point of primary drying in freeze-drying process control. *AAPS PharmSciTech* **2010**, *11*, 73–84.